Journal of Optics
https://doi.org/10.1007/s12596-024-01890-2

RESEARCH ARTICLE

Light emitting diodes based on carbon nanoparticles and Alq$_3$

Hussein Riyadh Mohammed[1] · **Asama N. Naje**[1]

Received: 28 March 2024 / Accepted: 2 May 2024

Abstract
The OI-LED device was fabricated using a combination of organic and inorganic semiconductors in multiple layers. This resulted has been improved generation of electroluminescence by incorporating carbon nanoparticles (with a size range of 20–40 nm) into materials such as poly (3, 4, -ethylene dioxythiophene) / polystyrene sulfonic acid (PEDOT: PSS), poly [(9, 9 – dioctylfluoreny l-2, 7- diyl)–co-(4, 4′-(N-(4-sec butylphenyl) diphenylamine)] (TFB and Tris (8-quinolinolato) aluminum(III) (Alq3). The fabrication process involved the use of spin coating technique and phase segregation method, which yielded thin film sample: (ITO/PEDOT: PSS/TFB/CNP/Alq3/AL). The electroluminescent properties of the OI-LED were investigated by interpreting the change resulting from applying different bias voltages 8, 9 and 10 V and the deposition of various organic layers at room temperature. The I-V curve clearly demonstrated the influence of the applied voltage on the knee voltages 1.7 V observed in sample. These characteristics enabled the OI-LED to emit a wide spectrum of light with wavelengths from 300 to 800 nm. It was calculated and studied color spaces by the Commission Internationale de l'Éclairage (Cie) 1931 system, and the correlated color temperature (CCT) of the device was found to range from 2000 to 3500 K.

Keywords Organic material · Carbon nanoparticle · Electroluminescence · Organic-inorganic light emitting diode

Introduction

In the past decades, silicon (Si), germanium (Ge) and their alloys have dominated the electronics industry, due to their unique properties [1]. However, there was significant progress in winners A. J. Heeger and G. MacDiarmid and H. Shirakawa in the late 1960s, when they were able to demonstrate the electrical conductivity of polyethylene, a conductive polymer (CP). This pioneering discovery eventually earned them a Nobel Prize [2]. Since semiconductors play an important role in our daily lives, extensive research in this field has led to the development of organic semiconductors with exceptional performance, thus revolutionizing electronic devices [3, 4]. These developments have high importance in important applications such as LEDs, solar cells, flexible displays, detectors, sensors, etc [5]. Scientists and researchers have been paying particular attention to (OLEDs) due to their various applications with high-intensity optical flat-panel displays attempts have been made to improve OLED performance by addressing issues such as injection barriers between organic materials and high-performance electrodes [6]. Organic matter is composed of molecules that interconnect, or polymers, consisting primarily of carbon and hydrogen atoms in complex assemblies. Occasionally, these materials may also include heterogeneous atoms like nitrogen. Organic materials are solid substances that consist of interconnected molecules or polymers. These materials primarily consist of carbon and hydrogen atoms, although other atoms such as nitrogen may also be present. Organic semiconductors exhibit an energy gap from 2 to 4 eV [7]. Initially, they are considered insulating materials rather than semiconductors. However, they can be rendered semiconductive through the injection of charge carriers via electrodes or by doping. The field of nanoscience and nanomaterials has led to significant advancements in the understanding of semiconductor materials at the nanoscale. This has resulted in the identification of distinct properties and characteristics of materials such as metal oxides and carbon compounds. Carbon, for instance, is a black charred substance with low solubility in water

---

✉ Hussein Riyadh Mohammed
h9389964@gmail.com

[1] College of Science, Physics Department, University of Baghdad, Baghdad, Iraq

and weak chemical interaction. It also exhibits unpromising photoluminescence [8]. Nevertheless, it was used utilization of chemical and physical methods for nagh thenostructures production for carbon transformation from an insulator to a semiconductor [9], carbon nanocomposites have been developed, which include Graphene Quantum Dot (GQD), Carbon Nanoparticles (CNP), Carbon Nanotubes (SWCNT, MWCNT) and others, which possess high solubility, chemical reactivity, and enhanced photoluminescence. These nanocomposites have shown great promise in the fabrication of inorganic emitting diodes [10]. The present study focuses on the achievement of electroluminescence by constructing hybrid light-emitting diodes composed of thin-film layers of organic and inorganic materials. These layers are sandwiched between two electrodes, with one electrode requiring transparency. Additional layers, such as the Hole Transporting Layer (HTL), Hole Injection Layer (HIL), Electron Transporting Layer (ETL), and Electron Injection Layer (EIL), aid in the injection and transfer of charge towards the CNP light-emitting layer [11, 12]. Furthermore, they contribute to the overall performance enhancement of the device. In this study, PEDOT: PSS and TFB were used to enhance (HTL) and (HIL), respectively, capabilities through the interlayer of hybrid light-emitting diode photovoltaic cells, while equip (ETL) from Alq3 which is known for high thermal stability and serves as an important mechanism in the emission level (EL) [13, 14]. OI-LED technology offers many advantages in devices a provides luminescent interior, including light weight, large area coverage, high flexibility, transparency, and low cost, these advantages vary. They are developed by thin-film deposition techniques obtain, such as vacuum thermal evaporation or spin coating, which will be discussed in detail in the practical Sect. [4]. Work is needed in fabricating organic and inorganic light-emitting diodes based on carbon nanoparticles to obtain light by the process of electro-luminesce on.

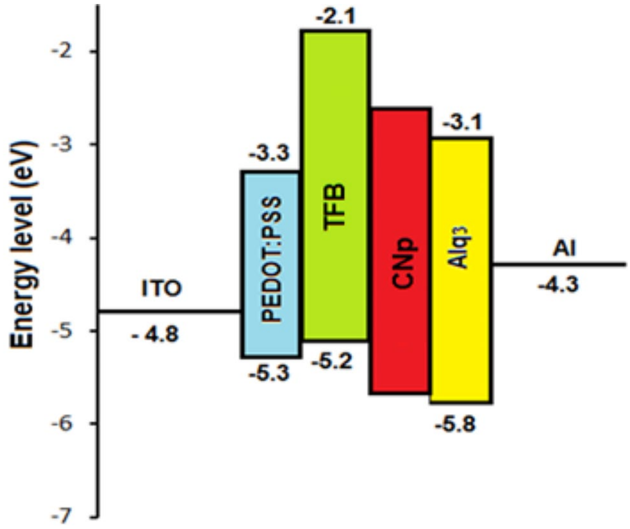

Fig. 1 Schematic diagram of diode device

Experimental procedure

The first step was carried out as shown in Fig. 1. First, the PEDOT: PSS solution was passed through a 0.45 µm PES filter into a darkened beaker. This precaution was necessary to avoid any change in the quality of the product due to light penetration [15]. In the second step, 10 mg of TFB was dissolved in 1 ml of chloroform solution using an ultrasonic device and a magnetic stir bar. Then, CNP was mixed with TFB in its weight ratio (x/300) to prepare it for use [13]. In the third step, 30 mg of Alq3 was dissolved in 3 ml of ethanol, a solution that does not affect or hydrolyze TFB. This dispersion process was implemented using an ultrasonic and a magnetic stirrer [16]. After molding, the final coating was applied to a conductive ITO layer of 2 × 2 cm^2 using the spin coating method. This allowed the precipitation of PEDOT: PSS by a distillation-diffusion process. The machine speed was then run at 1000 rpm, and the film was dried at 120 °C for 15 min and 50 °C for 1 h rpm, at 50 °C for 1 h, after that, the blend layer TFB: CNp was redeposited using a spin coating at 2000 rpm, then dried at a temperature of 50 °C for an hour, after which the Alq3 layer was deposited under the same conditions as the layer above [17, 18]. Finally, the multilayer hybrid film was completed (ITO/PEDOT: PSS/TFB/CNp/Alq3/AL).

Results and discussion

The absorption spectrum was analyzed in the range (300–800) nm, as shown in Fig. 2a–c, including absorption in the near ultraviolet (NUV) region.

Outside the NUV region, the absorption gradually decreased with increasing wavelength. The highest absorption peaks of TFB, Alq3, and CNP were at 428 nm, 396 nm, and 290 nm, respectively. Excitation wavelengths of 428, 396, and 290 nm were used to excite the samples and measure the photoluminescence (PL) of TFB, Alq3, and CNP [19], as shown in same figure, the energy gap (Eg) was determined using the equation Eg(eV) = 1240/λ(nm) for TFB, the first peak centered at 477 nm indicates a transition from the lowest unoccupied molecular orbital (LUMO) to the highest occupied molecular orbital (HOMO), indicating an energy difference of about 3 eV. Likewise for Alq3, the first peak centered at 520 nm indicates the transition from LUMO to HOMO, resulting in an energy gap of about 2.73 eV [20]. In addition, the energy gap between CNP was

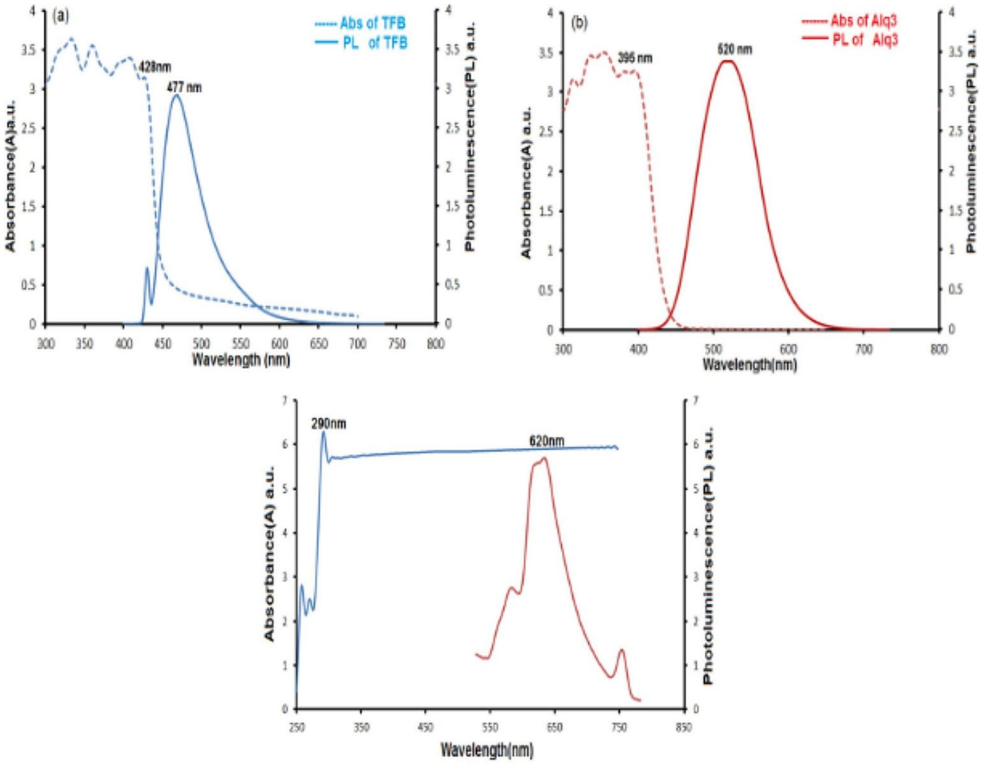

Fig. 2 Abs and PL (**a**) TFB (**b**) Alq$_3$ (**c**) CNp

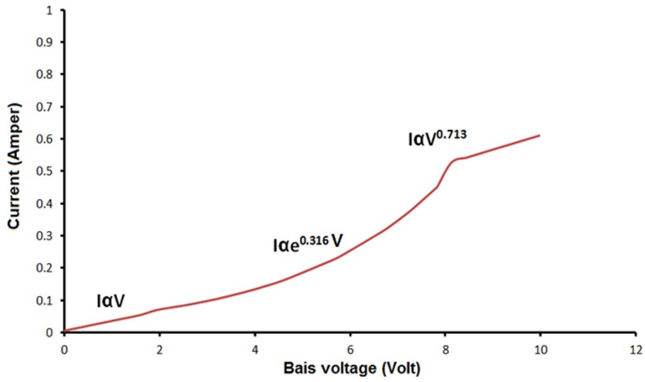

Fig. 3 I-V characteristics of multilayer devices

found to be about 2.2 eV due to the band-to-band difference at a wavelength of 620 nm [21].

The current-voltage relationship of a sample IO-LED device (ITO/PEDOT: PSS/TFB/CNp/Alq3/AL) was measured at room temperature. The results depicted in Fig. 3, illustrating the behavior of the current, which can be divided into three distinct stages. In stage 1 (voltage less than 2 V), the current as a function of voltage (IαV) showed a linear relationship, reflecting the flow of carriers through the low-voltage tunnels. The constant knee voltage of 1.7 V plays an important role at this stage. The stage 2, 2–8 V demonstrates an exponential increase in current values with respect to the applied voltage (Iα exp (X×V)), where X equals 0.316. This behavior is attributed to the varying ratio of injected carriers. It is worth noting that all voltage levels up to 8 V are considered filled voltage levels (VLFL). The expansion of stage 2 can be attributed to the low mobility of carriers in organic materials [16]. Finally, in stage 3; voltage greater than 8 V, the current as a function of voltage follows a power-law relationship (IαV^X), where X equals 0.713. It is during this stage that light emission begins, as the increase in bias voltage across the sample leads to a higher density of injected carriers concentration in the excited states of the organic layers. This in turn increases the Coulomb attraction, resulting in the emission of a spectrum of wavelengths [17].

The electroluminescence (EL) was measured at a forward bias voltage of 8, 9, and 10 V for the light passing through the sample. A spectrum of emission for the hybrid device was recorded by employing a photo-multiplier detector at room temperature. To enhance carrier transport, an additional layer was deposited due to the superior efficiency of transparent PEDOT: PSS among all conductive organic thermoelectric materials [19]. TFB and Alq3 were utilized for hole (h) and electron (e) injection and transport, respectively [22]. The anode ITO serves as a pathway for hole diffusion to the highest occupied molecular orbital (HOMO) of TFB and the valence band (V.B) of CNP. Conversely, aluminum cathodes inject and transfer electrons to the lowest unoccupied molecular orbital (LOMO) of Alq3 and the conduction band (C.B) of CNP. As a result of the injection process of (h) and (e) and the subsequent passage through the organic part, fusion occurs due to columbic attraction,

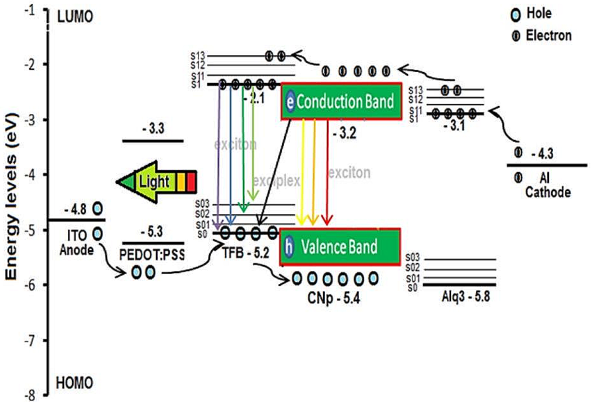

Fig. 4 Energy levels of a multilayer device ITO/PEDOT: PSS/TFB/CNp/Alq_3/AL [23, 24]

as depicted in Fig. 4. Consequently, the fusion of (h) and (e) leads to the formation of excitons and exciplex. Finally, a light source with multiple wavelengths is obtained .

Emission diagram was a results of the effect adding carbon nanoparticles(CNP) as an interlayer to the previously manufactured (O-LED) device (ITO/PEDOT: PSS/TFB / Alq3/AL) [19] led to the improvement, expansion and increase the intensity of the emission spectrum region due to the presence of sublevels which led to the emission shifting within the yellow, orange, and red region. The emission spectrum was obtained as a result of applying forward bias voltages 8, 9, and 10 V. These spectra were classified into three: the first the spectra 372, 395, 435 and 474 nm, resulting from the transition between the HOMO and LUMO levels of the TFB compound as a result of the formation of an exciton between them, the second the dominant spectra 506, 530, 542 and 568 nm, resulting from the transition between the valence band (V.B) and the conduction band (C.B) of carbon nanoparticles, the third the spectra 589, 599, 608, 630 and 688 nm, resulting from the generation of exciplex between the conduction band (C.B) of carbon nanoparticles and the HOMO levels of TFB. All these transitions are appearing in Fig. 5.

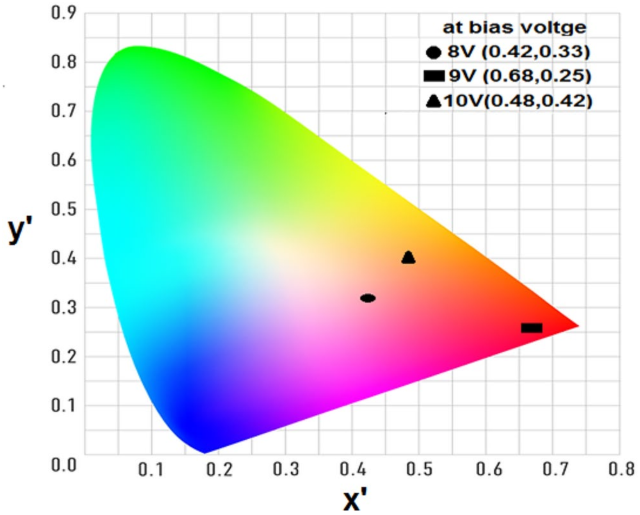

Fig. 6 Coordinates of a multilayer device in the CIE 1931 chromaticity diagram

Electroluminescence data were used the color of light is located by the Commission Internationale de l'Éclairage (Cie) 1931 Chromaticity Coordinate Fig. 6. The Coordinates x', y' is found from A, B and C:

$$x\prime = \frac{A}{A+B+C} \tag{1}$$

Where the A, B and C are area below the curve for red, green and blue are regions in EL spectrum, respectively.

Calculated CCT of light by using Mc-Camy's approximation polynomial to estimate the CCT from the x' and y' chromaticity coordinates as in Eq. 2 [25–27]:

$$CCT = -449\left(n^3\right) + 3525\left(n^2\right) - 6823\left(n\right) + 5520.33 \tag{2}$$

Fig. 5 EL at different bias forward voltages

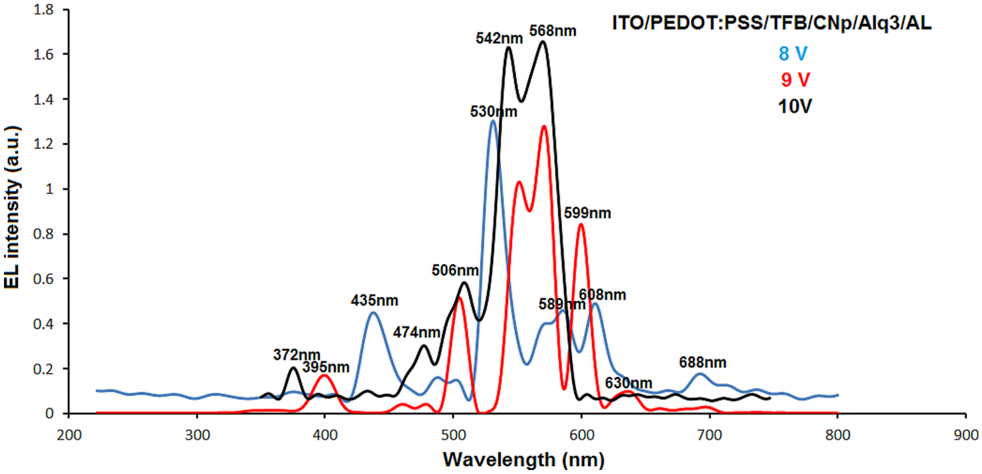

Table 1 CCT and x', y' coordinates for bias forward voltages

Simple	Voltage	x', y'	*n*	CCT (K)
ITO/PEDOT: PSS/TFB/CNp/Alq3/AL	8 V	0.42,0.33	0.7370	2206
//	9 V	0.68,0.25	0.7981	2064
//	10 V	0.48,0.42	0.4691	3043

where

$$n = (x' - 0.332)/(y' - 0.1855) \tag{3}$$

The all result can be tabulated in Table 1.

Conclusion

Based on the previous explanation, as the possibility of fabricating model of a hybrid LED from organic (PEDOT: PSS, TFB and ALq3) and inorganic (Carbon Nanoparticles (CNP)) multilayered thin films as a multi-wavelengths source at an bias forward voltage 8, 9 and 10 V, due to the transition between the levels of the HOMO and the LUMO of the organic compound or between C.B and V.B. of the inorganic compound forming an exciton, or the luminescence occurs as a result of the transitions between C.B, and the LUMO leading to the formation of an exciplex. One of the important results that occurred the effect of different organic layers on the intensity of light emission or shiftting of wavelengths, and thus calculating the correlated color temperature(CCT).

Author contributions Each co-author has made unique contributions to the work. The author **HRM** prepared the thin films and contributed to writing the article draft and wrote the program for optical properties and contributed to the analysis of the results. As the author **ANN**, he supervised the work and reviewed the article draft.

Funding information The authors have not disclosed any funding.

Data availability Data sharing is not applicable to this article as no datasets were created or analyzed during the current study.

Declarations

Ethical approval The authors would like to declare that they do not have any conflict of interests.

Competing interests The authors have not disclosed any competing interests.

References

1. Wolfgang, Brütting, Introduction to the physics of organic semiconductors, Physics of organic semiconductors, 1–14 (2005)
2. Lakshmanan, S.C.G. Kiruba, Daniel, Engineered nanomaterials for organic light-emitting diodes (OLEDs), Handbook of nanomaterials for industrial applications, 312–323 (2018)
3. B. Lüssem, M. Riede, K. Leo, Doping of organic semiconductors. Phys. Status Solidi A **210**(1), 9–43 (2013)
4. H. He, Applications in OLED and QLED, Solution Processed Metal Oxide Thin films for Electronic Applications, 141–154 (2020)
5. P.-A. Will, S. Reineke, *Organic light-emitting Diodes, Handbook of Organic Materials for Electronic and Photonic Devices* (Woodhead Publishing, 2019), pp. 695–726
6. M.C. Gather, A. Köhnen, K. Meerholz, White organic light-emitting diodes. Adv. Mater. **23**(2), 233–248 (2011)
7. B. Geffroy, P.L. Roy, C. Prat, Organic light-emitting diode (OLED) technology: materials, devices and display technologies. Polym. Int. **55**(6), 572–582 (2006)
8. Y. Wang, A. Hu, Carbon quantum dots: synthesis, properties and applications. J. Mater. Chem. C **34**, 6921–6939 (2014)
9. A.H. Abd, O.A. Ibrahim, Synthesis of Carbon Quantum dot by Electro-Chemical Method and Studying Optical Electrical and Structural properties. Chem. Methodol. **6**(11), 823–830 (2022)
10. A.H. Mohammed, A.N. Naje, R.K. Ibrahim, Photoconductive detector based on Graphene Doping with Silver Nanoparticles. Iraqi J. Sci. **63**(12), 5218–5231 (2022)
11. P. Li, Z.-H. Lu, Interface Engineering in Organic electronics: Energy-Level Alignment and Charge Transport. Small Sci. **1**(1), 2000015 (2021)
12. G.M. Farinola, R. Ragni, Electroluminescent materials for white organic light emitting diodes. Chem. Soc. Rev. **40**, 3467–3482 (2011)
13. A.R. Rodrigues, W. Novais, Renzi, Neusmar Junior Artico Cordeiro, Edson Laureto, Ivan Frederico Lupiano Dias, and José Leonil Duarte, Study of energy transfer in polymer blends of TFB: P3HT, Semina. Exact Technological Sci. **38**(1), 91–100 (2017)
14. V.A. Dediu, L.E. Hueso, I. Bergenti, C. Taliani, Spin routes in organic semiconductors. Nat. Mater. **8**(9), 707–716 (2009)
15. H.R. Mohammed, O.A. Ibrahim, Electroluminescence of light-emitting Organic Semiconductor/Europium Oxide Nanoparticle Hybrid Junction. Iraqi J. Sci. **61**(8), 1952–1959 (2020)
16. H.R. Mohammed, O.A. Ibrahim, Preparation of Hybrid Junction Light emitting device from Cadmium Sulphite Quantum dot/poly-TPD Junction, University of Thi-Qar. J. Sci. **8**(2), 100–103 (2021)
17. H.R. Mohammed, Fabrication of electroluminescence device for PEDOT: PSS/ploy TPD/Eu2O3 nanoparticles junction. Iraqi J. Phys. **17**(43), 33–40 (2019)
18. A.M. Kadim, O.A. Ibrahim, W.R. Saleh, Electroluminescence devices from quantum dots with TPD polymer white light generation. J. Nano Res. **48**, 104–113 (2017)
19. L.A. Essa, R.K. Jamal, Studying the structural and optical properties of carbon quantum dots prepared by electro–chemical method. J. Opt., https://doi.org/10.1007/s12596-023-01328-1
20. T. Hoshi, K.-I. Kumagai, K. Inoue, S. Enomoto, Y. Nobe, M. Kobayashi, Electronic absorption and emission spectra of Alq3 in solution with special attention to a delayed fluorescence. J. Lumin. **128**(8), 1353–1358 (2008)
21. Z. Wang, N. Jiang, M. Liu, R. Zhang, F. Huang, D. Chen, Bright Electroluminescent White-Light-emitting diodes based on

Carbon dots with tunable correlated color temperature enabled by aggregation. Small. **17**(52), 2104551 (2021)

22. M. Auer-Berger, R. Trattnig, T. Qin, R. Schlesinger, M.V. Nardi, G. Ligorio, C. Christodoulou, N. Koch, M. Baumgarten, K. Mullen, All-solution-processed multilayer polymer/dendrimer light emitting diodes. Org. Electron. **35**, 164–170 (2016)
23. J.H. Lee, C.-H. Chen, P.H. Lee, H.Y. Lin, M. –, K. Leung, T.L. Chiu, C. –, F. Lin, Blue organic light-emitting diodes: current status, challenges, and future outlook. J. Mater. Chem. C **7**(20), 5874–5888 (2019)
24. P. Xiao, T. Dong, J. Xie, D. Luo, J. Yuan, B. Liu, Emergence of white organic light-emitting diodes based on thermally activated delayed fluorescence. Appl. Sci. **8**(2), 299 (2018)
25. O.A. Ibrahim, A.M. Kadim, W.R. Saleh, White Light Generation from Electroluminescence Devices Using TPD: PMMA/QDs/Alq3, Nano Hybrids and Composites, 15, 10–20 (2017)
26. C.S. McCamy, Correlated color temperature as an explicit function of chromaticity coordinates. Color. Res. Application. **17**(2), 142–144 (1992)
27. A.N. Naje, O.A. Ibrahim, E.T. Abdullah, Blue Organic-Inorganic Light Emitting Diode based on Electroluminescence CdS nanoparticle. Iraqi J. Sci. **64**(12), 6277–6284 (2023)